We are IntechOpen,
the world's leading publisher of
Open Access books
Built by scientists, for scientists

6,900
Open access books available

185,000
International authors and editors

200M
Downloads

154
Countries delivered to

Our authors are among the

TOP 1%
most cited scientists

12.2%
Contributors from top 500 universities

CLARIVATE ANALYTICS

BOOK CITATION INDEX

INDEXED

WEB OF SCIENCE™

Selection of our books indexed in the Book Citation Index
in Web of Science™ Core Collection (BKCI)

Interested in publishing with us?
Contact book.department@intechopen.com

Fast Kinetic Methods with Photodiode Array Detection in the Study of the Interaction and Electron Transfer Between Flavodoxin and Ferredoxin NADP⁺-Reductase

Ana Serrano and Milagros Medina
*Department of Biochemistry and Molecular and Cellular Biology and Institute of
Biocomputation and Physics of Complex Systems, University of Zaragoza
Spain*

1. Introduction

The primary function of Photosystem I (PSI)[1] during photosynthesis is to provide reducing equivalents, in the form of NADPH, that will then be used in CO_2 assimilation (Golbeck, 2006). In plants, this occurs via reduction of the soluble [2Fe-2S] Ferredoxin (Fd) by PSI. Subsequent reduction of $NADP^+$ by Fd_{rd} is catalysed by the FAD-dependent Ferredoxin-$NADP^+$ reductase (FNR) ($E_{ox/hq}$ = -374 mV at pH 8.0 and 25°C) through the formation of a ternary complex (Arakaki *et al.*, 1997; Nogués *et al.*, 2004; Sancho *et al.*, 1990). In most cyanobacteria and some algae under low iron conditions the FMN-dependent Flavodoxin (Fld), particularly its Fld_{sq}/Fld_{hq} couple ($E_{ox/sq}$ = -256 mV, $E_{sq/hq}$ = -445 mV at pH 8.0 and 25°C), substitutes for the Fd_{ox}/Fd_{rd} pair in this reaction (Bottin & Lagoutte, 1992; Goñi *et al.*, 2009; Medina & Gómez-Moreno, 2004). Thus, two Fld_{hq} molecules transfer two electrons to one FNR_{ox} that gets fully reduced after formation of the FNR_{sq} intermediate. FNR_{hq} transfers then both electrons simultaneously to $NADP^+$ (Medina, 2009) (Figure 1).

Additionally to their role in photosynthesis, Fld and FNR are ubiquitous flavoenzymes that deliver low midpoint potential electrons to redox-based metabolisms in plastids, mitochondria and bacteria in all kingdoms (Müller, 1991). They are also basic prototypes for a large family of di-flavin electron transferases that display common functional and structural properties, where the electron transfer (ET) flow supported by the Fld/FNR modules occurs in reverse direction to the photosynthesis (Brenner *et al.*, 2008; Wolthers & Scrutton, 2004). The better understanding of the ET flavin-flavin mechanism in this system should witness a greater comprehension of the many physiological roles that Fld and FNR, either free or as modules in multidomain proteins, play. In these chains there are still many

---

[1] PSI, Photosystem I; FNR, ferredoxin-$NADP^+$ reductase; FNR_{ox}, FNR in the fully oxidised state; FNR_{sq}, FNR in the semiquinone state; FNR_{hq}, FNR in the hydroquinone (fully reduced) state; Fld, Fladoxin; Fld_{ox}, Fld in the fully oxidised state; Fld_{sq}, Fld in the semiquinone state; Fld_{hq}, Fld in the hydroquinone (fully reduced) state; Fd, ferredoxin; Fd_{ox}, Fd in the oxidised state; Fd_{rd}, Fd in the reduced state; $E_{ox/sq}$, midpoint reduction potential for the ox/sq couple; $E_{sq/hq}$, midpoint reduction potential for the sq/hq couple; ET, electron transfer; WT, wild-type; $k_{A\to B}$, $k_{B\to C}$, $k_{C\to D}$, apparent rate constants obtained by global analysis of spectral kinetic data; I, ionic strength; UV/Vis, ultraviolet/visible; PDA, photodiode array detector; SVD, single value decomposition.

open questions in understanding not only the ET mechanisms, but also the role that the flavin itself might play.
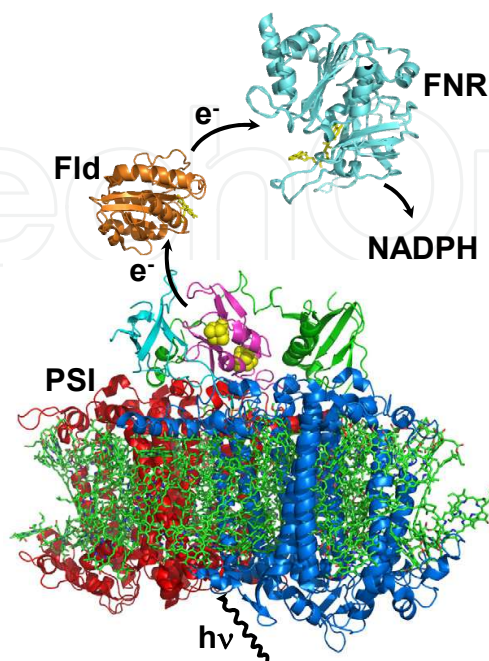

Fig. 1. Proteins involved in the photosynthetic electron transfer from PSI to NADP+ via Flavodoxin (Fld, orange) and Ferredoxin-NADP+ reductase (FNR, blue).

Recent studies on the FNR:Fld interaction and ET indicate that the orientation driven by the alignment of the Fld molecular dipole moment with that of FNR contributes to the formation of a bunch of alternative binding modes competent for the efficient ET reaction (Frago *et al.*, 2010; Goñi *et al.*, 2009; Medina *et al.*, 2008). FNR, Fld and NADP+ are able to form a ternary complex, indicating that NADP+ is able to occupy a site on FNR without displacing Fld (Martínez-Júlvez *et al.*, 2009; Velázquez-Campoy *et al.*, 2006). The two binding sites are not completely independent, and the overall reaction is expected to work in an ordered two-substrate process, with the pyridine nucleotide binding first, as reported for the Fd system (Batie & Kamin, 1984a, 1984b). Complex formation of Fd_{rd} with FNR:NADP+ was found to increase the ET rate by facilitating the rate-limiting step of the process, the dissociation of the product (Fd_{ox}) (Carrillo & Ceccarelli, 2003). Binding equilibrium and steady-state studies in WT and mutant proteins envisaged similar mechanisms for Fld, but the less specific FNR:Fld interaction might alter this behaviour (Medina, 2009).

Fast kinetic stopped-flow methods have been used for the analysis of the mechanisms involving binding and ET between FNR and Fld. So far only single wavelength stopped-flow spectrophotometry studies (mainly at 600 nm) have been reported (Casaus *et al.*, 2002; Goñi *et al.*, 2008; Goñi *et al.*, 2009; Nogués *et al.*, 2003; Nogués *et al.*, 2005), not involving the effects of NADP+, the ionic strength of the media, or the evaluation of the intermediate and final compounds of the equilibrium mixture. In this work, we use stopped-flow with photodiode array detection (PDA) to better evaluate the intermediate and final species in the equilibrium mixture during the ET process in the binary Fld:FNR and ternary Fld:FNR:NADP+ systems.

2. Experimental methods improving the kinetic analysis of pre-steady-state electron transfer processes

ET has been analysed at different ionic strengths (I) and in both directions; the physiological photosynthetic ET, from Fld$_{hq}$ to FNR$_{ox}$, and the reverse ET, from FNR$_{hq}$ to Fld$_{ox}$, used to provide reducing equivalents to different metabolic pathways. Different *Anabaena* FNR and Fld variants have been used in the kinetic characterization of these ET processes using stopped-flow with photodiode detection.

2.1 Biological material and steady-state spectroscopic measurements

The different FNR and Fld variants were purified from *Luria-Bertani* IPTG-induced *E. coli* cultures containing, respectively, the pTrc99a-Fld and pET28a-FNR plasmids encoding *Anabaena* WT or E301A FNRs and WT, E16K/E61K or E16K/E61K/D126K/D150K Flds as previously described (Casaus *et al.*, 2002; Goñi *et al.*, 2009; Martínez-Júlvez *et al.*, 2001; Medina *et al.*, 1998; Tejero *et al.*, 2003). UV/Vis spectra were recorded in a Cary 100 spectrophotometer at 25 °C. Unless otherwise stated, all measurements were recorded in 50 mM Tris/HCl, pH 8.0. Binding ability between WT FNR$_{ox}$ and WT Fld$_{ox}$ was determined using difference absorption spectroscopy as previously described (Goñi *et al.*, 2009; Martínez-Júlvez *et al.*, 2001; Medina *et al.*, 1998).

2.2 Stopped-flow pre-steady-state kinetic measurements

Fast ET processes between Fld and FNR were followed by stopped-flow under anaerobic conditions in 50 mM Tris/HCl, pH 8.0 at 12°C. Reactions were analysed by collecting multiple wavelength absorption data (360-700 nm) using an Applied Photophysics SX17.MV stopped-flow and a photodiode array detector (PDA) with the X-Scan software (*App. Photo. Ltd.*). Typically, 400 spectra *per* second were collected for each reaction. Anaerobic conditions were obtained by several cycles of evacuation and bubbling with O$_2$-free argon. FNR$_{hq}$ and Fld$_{hq}$ samples were obtained by photoreduction in the presence of 1 mM EDTA and 5 µM 5-deazariboflavin (Medina *et al.*, 1998). The use of PDA allowed detecting that under our experimental conditions the produced Fld$_{hq}$ samples usually contained a small amount of Fld$_{sq}$ (detected at ~580 nm), taken into account in subsequent analysis. Unless otherwise stated, the mixing molar ratio was 1:1 with a final concentration of 10 µM for each protein. Molar ratios of 1:1, 1:2, 1:4 and 1:8 were also assayed for the reaction of FNR$_{hq}$ and Fld$_{ox}$, with a final FNR$_{hq}$ concentration of 10 µM. Reactions were also analysed at different ionic strengths, obtained using variable NaCl concentrations ranging from 0 to 300 mM in 50 mM Tris/HCl, pH 8.0. The reaction between FNR$_{ox}$ and Fld$_{hq}$ was also studied in presence of ~300 µM NADP$^+$ at the indicated ionic strength conditions.

2.3 Kinetic analysis of multiple-wavelength absorption data

Spectral intermediates formed during reactions were resolved by singular value decomposition (SVD) using Pro-Kineticist (*App. Photo. Ltd.*). Data collected were fit either to a single step, A→B, to a two steps A→B→C, or to a three steps, A→B→C, model allowing estimation of the conversion rate constants ($k_{A→B}$, $k_{B→C}$, $k_{C→D}$) (Tejero *et al.*, 2007). Estimated errors in the determined rate constant values were ±15%. It should be stressed that SVD analysis of PDA spectra over a selected time domain resolves the spectra in the minima number of spectral intermediates species that are formed during the reaction, reflecting a

distribution of protein intermediates (reactants, complexes, products...) at a certain point along the reaction time course, and not discrete enzyme intermediates. Moreover, none of them represent individual species and, their spectra cannot be included as fixed values in the global-fitting. Consequently, a spectral intermediate, in particular one that is formed in the middle of a reaction sequence, is an equilibrium distribution of protein species that are formed in a resolvable kinetic phase. Model validity was assessed by lack of systematic deviation from the residual plot at different wavelengths, inspection of calculated spectra and consistence among the number of significant singular values with the fit model. Simulations using Pro-Kineticist were also performed in order to validate the determined ET kinetics constants for the direct and reverse processes.

2.4 Determination of the absorbance spectra of FNR_{sq} and Fld_{sq}, and of protein discrete species contained in the spectral intermediates

Due to the high maximum level for Fld_{sq} stabilisation, the spectrum from this species was easily determined from photoreduction experiments (Fig. 2A) (Frago *et al.*, 2007). The spectrum of FNR_{sq} was determined by following the one-electron oxidation of FNR_{hq} with ferricyanide in the spectral range between 360 and 700 nm (Batie & Kamin, 1984a). Molar ratios FNR_{hq}:ferricyanide of 1:10, 1:15 and 1:20 were used, with a final FNR_{hq} concentration of 10 μM (Fig. 2B). Analysis of the spectroscopic data along the time was performed by Multivariate Curve Resolution-Alternating Least Squares (MCR-ALS).

Intermediate A, B, C and D species were deconvoluted initially considering they are produced by the lineal combination of FNR_{ox}, FNR_{sq}, FNR_{hq}, Fld_{ox}, Fld_{sq} and Fld_{hq} spectra (Fig. 2), and having into account the mass balance for total FNR and Fld. Deviations from the linear combination of the different redox states of FNR and Fld were observed in all cases. Visible spectra of FNR-Fld reaction mixtures slightly differ from the lineal combination of the individual components due to modulation of the flavin spectroscopic properties when changing its environment polarity upon complex formation. This indicates contribution of FNR:Fld complexes to the spectra of intermediate and final species (Casaus *et al.*, 2002; Martínez-Júlvez *et al.*, 2001; Nogués *et al.*, 2003). Nevertheless, simulations proved that the method was adequate to estimate the percentage of the different redox states of each protein.
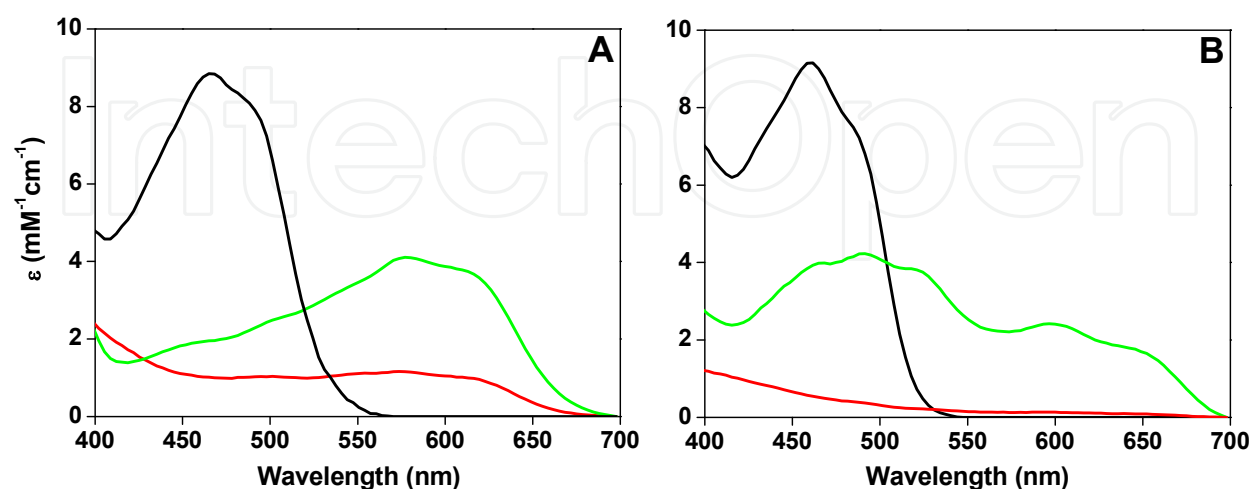

Fig. 2. Extinction coefficient of (A) Fld and (B) FNR in their different oxidation states. Oxidised, semiquinone and, reduced species are shown in black, green and red, respectively.

3. Spectral evolution of the electron transfer from Fld_{hq} to FNR_{ox}

Mixing Fld_{hq} with FNR_{ox} at I ≤ 125 mM produced a slight increase in the global amount of neutral semiquinone species within the instrumental dead-time. Then, absorbance decreased in the region of the flavin band-I (458 and 464 nm), while additionally increased in the 507-650 nm range (Fig. 3A and 3B). The overall reaction best fits a single ET step (described by an apparent $k_{B \to C}$ rate constant), without detection of a protein-protein interaction step ($k_{A \to B}$). Resolution of the spectroscopic properties of B was consistent with FNR_{ox} and Fld_{hq} as the main components, while those of the final species C indicated Fld accumulated mainly as Fld_{sq}, while FNR consisted mainly of FNR_{ox} (80%) in equilibrium with smaller amounts of FNR_{sq} and FNR_{hq} (~10% each). Deviation of the lineal combination of the
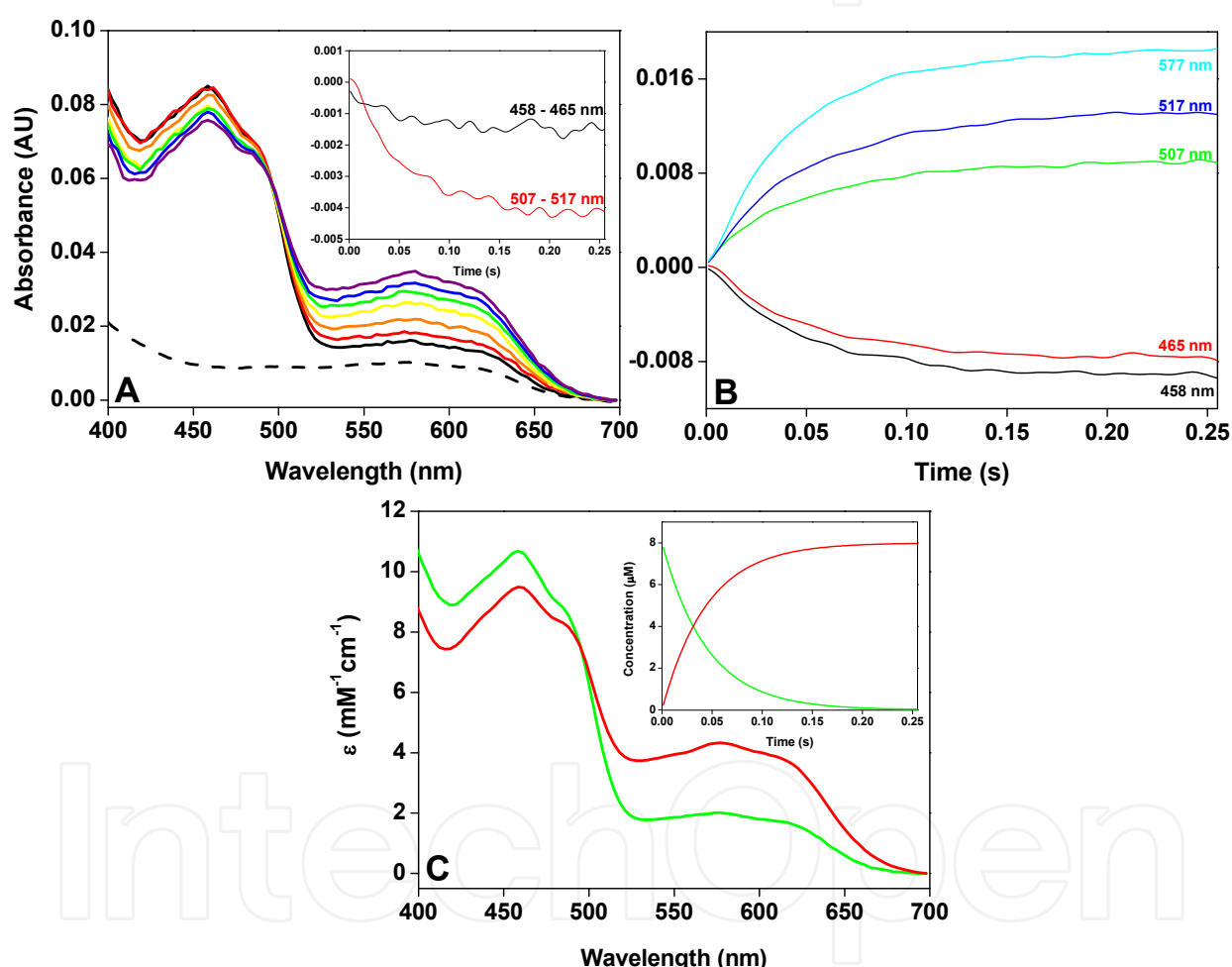

Fig. 3. Evolution of spectral changes during the reaction of Fld_{hq} with FNR_{ox} in 50 mM Tris/HCl, pH 8.0, 100 mM NaCl at 12ºC. (A). Time course for the reaction. Spectra recorded at 0.00128, 0.0064, 0.01664, 0.03712, 0.05504, 0.0832 and, 0.2547 s after mixing. The spectrum of Fld_{hq} before mixing is shown as a dashed line, and the first spectrum after mixing is in black. The inset shows differences between kinetic traces at the indicated wavelengths. (B). Kinetics of the absorbance changes at 458, 464, 507, 517 and 577 nm. (C). Absorbance spectra for the pre-steady-state kinetically distinguishable species obtained by global analysis. Intermediate B and C species are shown in green and red lines, respectively. The inset shows the evolution of these species along the time.

different FNR and Fld redox spectra was observed for B and C (Fig. 2), indicating mutual modulation of the spectroscopic properties of each one of the flavins, and, therefore, of its environment, by the presence of the second flavoprotein. This indicates a number of molecules must be forming FNR:Fld interactions, which might even be in different oxido-reduction states.

Noticeably, increasing ionic strength up to 125 mM had a drastic deleterious impact in the ET apparent $k_{B \to C}$ rate constant (Fig. 4), consistent with the lack of interaction observed by difference spectroscopy when WT FNR_{ox} was titrated with WT Fld_{ox} at I = 125 mM (not shown). These results indicated a considerable decrease in the FNR:Fld affinity upon increasing the ionic strength of the media.
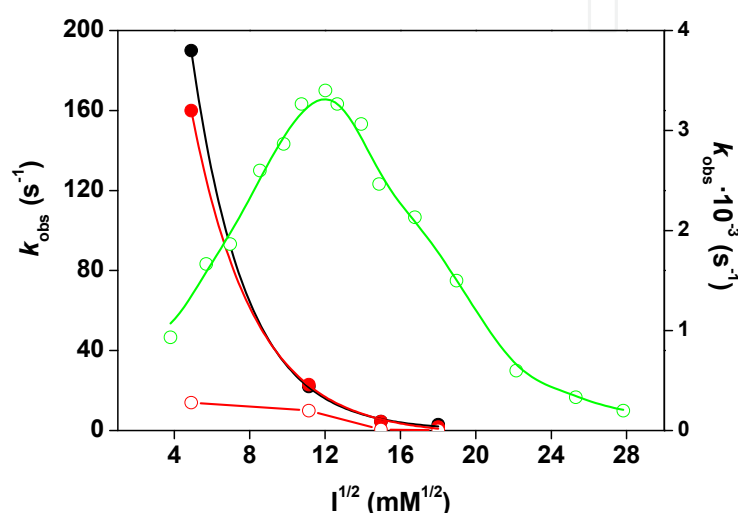

Fig. 4. Ionic strength dependence of the apparent rate constants for the reduction of FNR_{ox} by Fld_{hq} in absence (black) and presence of $NADP^+$ (red). $k_{B \to C}$ rate constants in absence (black closed circles) and in presence (red closed circles) of $NADP^+$. $k_{C \to D}$ rate constant in presence of $NADP^+$ (red open circles). The ionic strength profile reported for the reduction of FNR_{ox} by Fd_{rd} is plotted on the right axis of the figure (open green circles) (Medina et al., 1998).

Further increases in the ionic strength (I > 225 mM) produced the appearance of an additional final slow absorbance increase in the band-I, and, therefore, two ET steps described the process (Fig. 5). Thus, a slight absorbance bleaching of the band-I was observed from species B into C (as before described at lower I), but C further evolved with absorbance increases of this band and minor changes in the semiquinone one (Fig. 5A and 5C). Resolution of the spectroscopic properties of B was also consistent with FNR_{ox} and Fld_{hq} as the main components, those of C indicated Fld_{sq} and FNR_{ox} in equilibrium with some amounts of FNR_{sq} (~10%), and FNR_{hq} (~20%), while D was mainly composed by Fld_{sq} and FNR_{ox} with ~15% of Fld_{ox} and FNR_{hq}. The ionic strength additionally contributed to considerably diminish the apparent $k_{B \to C}$ ET rates (Fig. 4).

ET from Fld_{hq} to the $FNR_{ox}:NADP^+$ preformed complex was consistent with two ET steps at all the assayed ionic strengths, and the presence of the pyridine nucleotide apparently modulated the electronic properties of the flavins (compare Fig. 6 with 3A and 3C). These observations correlated with the changes produced in the FNR spectrum upon $NADP^+$ complexation (Tejero et al., 2005). Despite the presence of $NADP^+$ barely affected apparent $k_{B \to C}$ between Fld and FNR (Table 1, Fig. 4), C showed increments in both the semiquinone

and the band-I of the flavin with regard to B. The different spectroscopic properties of the intermediate species in the absence and presence of the nucleotide suggests that the nicotinamide portion of NADP⁺ must contribute to the catalytically competent active site, probably by modulating the orientation and/or distance between the reacting flavins. This is in agreement with the negative cooperative effect observed for simultaneous binding of Fld and NADP⁺ to FNR (Velázquez-Campoy *et al.*, 2006). Additionally, C slowly evolved with a slight absorbance increase at the band-I of the flavin with minor changes in the semiquinone. These observations still indicate initial production of Fld_{sq} and reduction of FNR_{ox}, but suggest an additional step consistent with further FNR reoxidation. Analysis of the kinetic traces at 340 nm, where absorbance increase upon reduction of NADP⁺ to
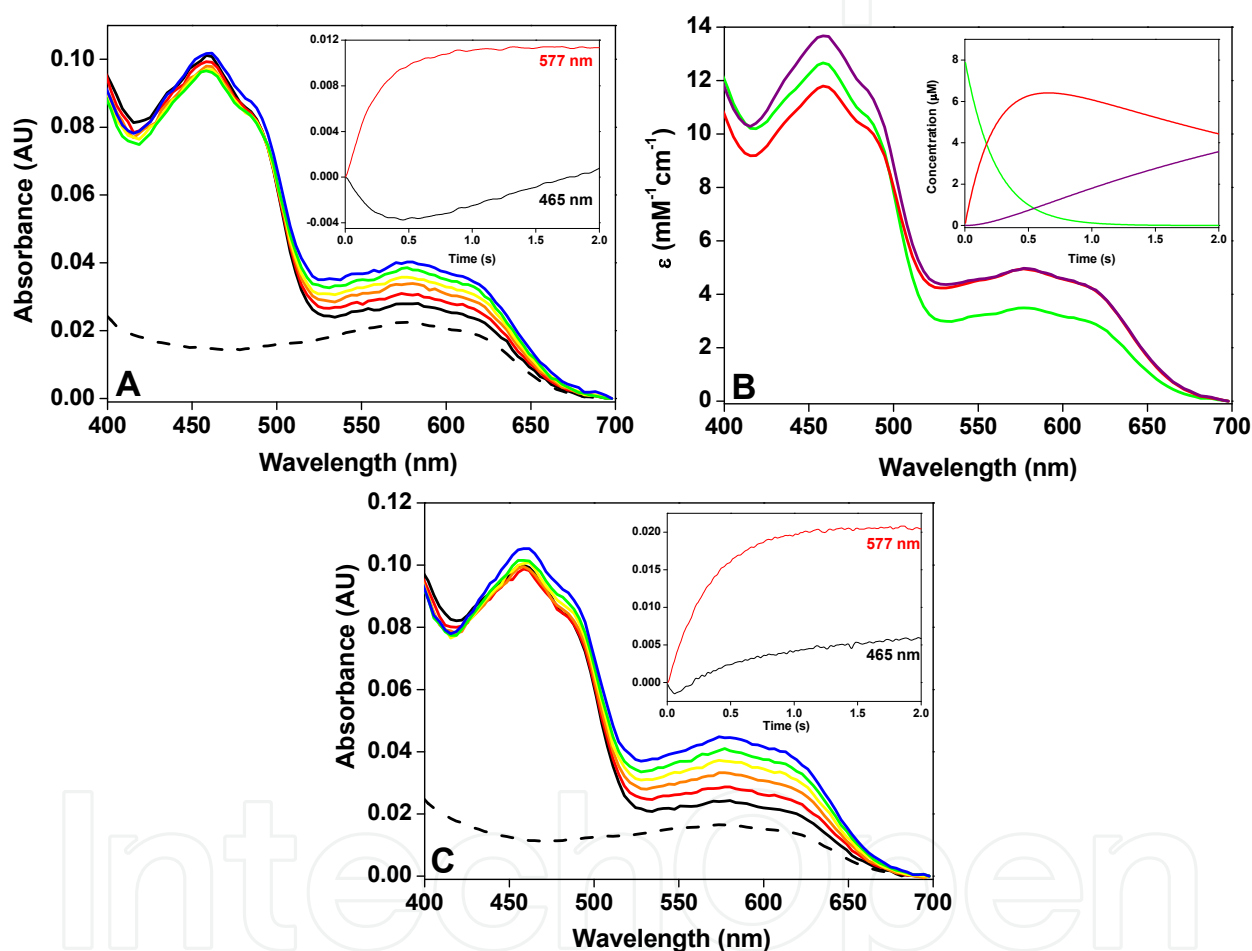

Fig. 5. Ionic strenght dependence of spectral evolution. (A). Time course for the reaction Fld_{hq} with FNR_{ox} in 50 mM Tris/HCl, pH 8.0, 200 mM NaCl at 12°C. Spectra recorded at 0.00384, 0.007552, 0.1626, 0.265, 0.5514 and, 2.047 s after mixing. The inset shows kinetic traces at the indicated wavelengths. (B). Absorbance spectra for the pre-steady-state kinetically distinguishable species obtained by global analysis of the reaction in A. The inset shows the species evolution along the time. B, C, and D species are shown in green, red and purple lines, respectively. (C). Time course for the reaction at 300 mM NaCl. Spectra recorded at 0.00384, 0.08576, 0.2035, 0.3315, 0.5158 and, 2.047 s after mixing. The inset shows kinetic traces at the indicated wavelengths. In A and C, the spectra corresponding to the Fld_{hq} before mixing are shown as a dashed line, and the first spectra after mixing are in black.

NADPH is expected, shows that amplitudes are considerably larger for samples containing the coenzyme (not shown). This indicates the last detected step must be related with the hydride transfer from FNR_{hq} to $NADP^+$ to produce its reduced form. Additionally, while the ionic strength of the media decreases the amplitudes at 340 nm for the reactions in the absence of $NADP^+$, those in its presence are nearly unaffected (not shown).

This process was also analysed for some FNR or Fld mutants previously produced and showing altered interaction or ET properties. This includes the FNR variant produced when Ala substituted for E301, a residue involved in the FNR catalytic mechanism as proton donor as well as for the stabilisation of reaction intermediates (Dumit *et al.*, 2010; Medina *et al.*, 1998). Analysis of the reduction of this variant by WT Fld_{hq} using the PDA detector showed that most of the ET took place within the instrumental dead time (not shown), confirming this is a very fast process as previously suggested (Medina *et al.*, 1998). Moreover, in contrast to the WT process, no changes in rate constants or species were observed upon increasing the ionic strength of the media (Table 1). Thus, only information of the final spectra was obtained, being this similar to those for the WT reaction with main accumulation of Fld_{sq} and FNR_{ox}. In the presence of $NADP^+$ production of NADPH was observed at 340 nm with similar rates to those reported for the WT reaction.
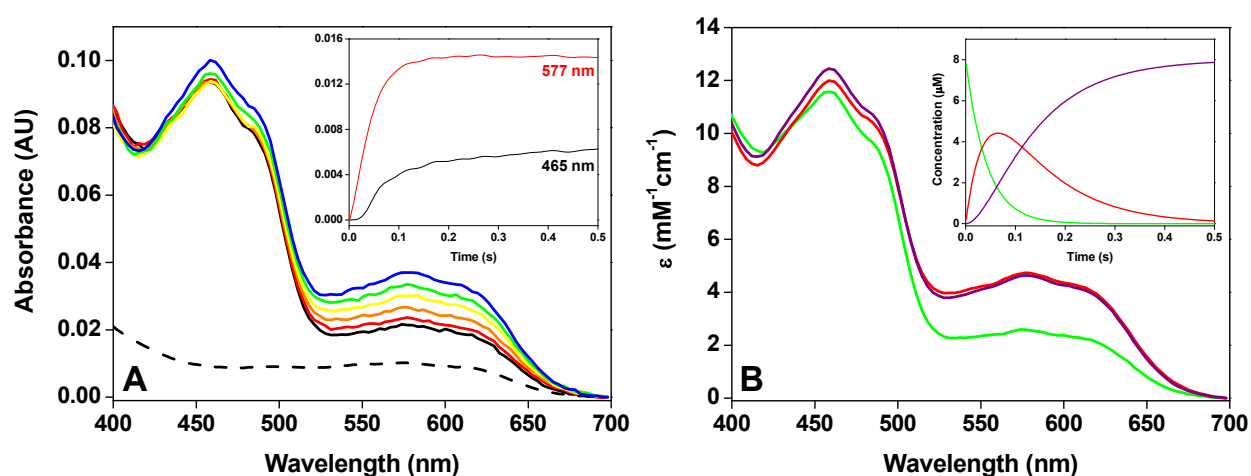

Fig. 6. Evolution of spectral changes during the reaction of Fld_{hq} with FNR_{ox} in 50 mM Tris/HCl, pH 8.0, 100 mM NaCl at 12ºC and $NADP^+$ ~300 μM. (A). Time course for the reaction. Spectra recorded at 0.00128, 0.0064, 0.01664, 0.03712, 0.05504 and, 0.5107 s after mixing. The inset shows kinetic traces at the indicated wavelengths. (B). Absorbance spectra for the pre-steady-state kinetically distinguishable species obtained by global analysis. The inset shows the evolution of these species along the time. Species B, C and D are shown in green, red and purple lines, respectively.

The process was similarly analysed for two Fld mutants for which the interaction step with FNR was reported to be modified by the introduction of multiple mutations (Goñi *et al.*, 2009). Spectral evolution for the ET process between E16K/E61K Fld_{hq} and FNR_{ox} at low ionic strength (I = 25 mM) presented similar features to those above described for WT Fld (not shown). Despite a similar starting behaviour was observed for the reaction of E16K/E61K/D126K/D150K Fld_{hq}, final absorbance increase and decrease in the flavin I and semiquinone bands, respectively, were observed (not shown). In both cases, but particularly with E16K/E61K/D126K/D150K Fld_{hq}, evolution of the system was considerably hindered.

Despite process for E16K/E61K Fld_{hq} fits a single ET step, with B showing similar characteristics to those in the WT reaction, a 17-fold decrease in $k_{B\rightarrow C}$ was observed (Table 1, Fig. 7A). Moreover, the final species C showed the appearance of Fld_{ox} (25%) in equilibrium with Fld_{sq} (75%), while the amount of FNR_{ox} (40%) decreased with regard to the WT reaction with the consequent increase in the proportions of FNR_{sq} (20%) and FNR_{hq} (40%). The process for E16K/E61K/D126K/D150K Fld_{hq} fits a two ET model, with $k_{B\rightarrow C}$ being hindered up to 190-fold with regard to WT (Table 1, Fig. 7B). Surprisingly, C shows important amounts of the reduced species of both proteins and its additional transformation is consistent with Fld_{sq} and FNR_{hq} as the main products of the reaction. For both Fld mutants the increase in the ionic strength again had deleterious kinetic effects in the overall ET (Table 1).

FNR form	Fld form	I (mM)	FNR_{ox} + Fld_{hq}		FNR_{hq} + Fld_{ox}	
			$k_{B\rightarrow C}$ (s^{-1})	$k_{C\rightarrow D}$ (s^{-1})	$k_{B\rightarrow C}$ (s^{-1})	$k_{C\rightarrow D}$ (s^{-1})
WT	WT	25	190[a]		2.0	0.5
WT	WT	125	22		0.7	0.3
E301A	WT	25	>300[a]		0.4	0.1
E301A	WT	125	>300[a]		0.4	0.03
WT:NADP$^+$	WT	25	160	14		
WT:NADP$^+$	WT	125	23	10		
WT	E16K/E61K	25	11.3		0.9	0.3
WT	E16K/E61K	125	<0.005		1.4	0.3
WT	E16K/E61K/D126K/D150K	25	1.0	0.4	1.2	0.1
WT	E16K/E61K/D126K/D150K	125	<0.005		<0.001	

Table 1. Kinetic parameters for the electron transfer between *Anabaena* Fld and FNR variants determined by stopped-flow and PDA detection. [a]Most of the reaction took place in the instrumental dead time.
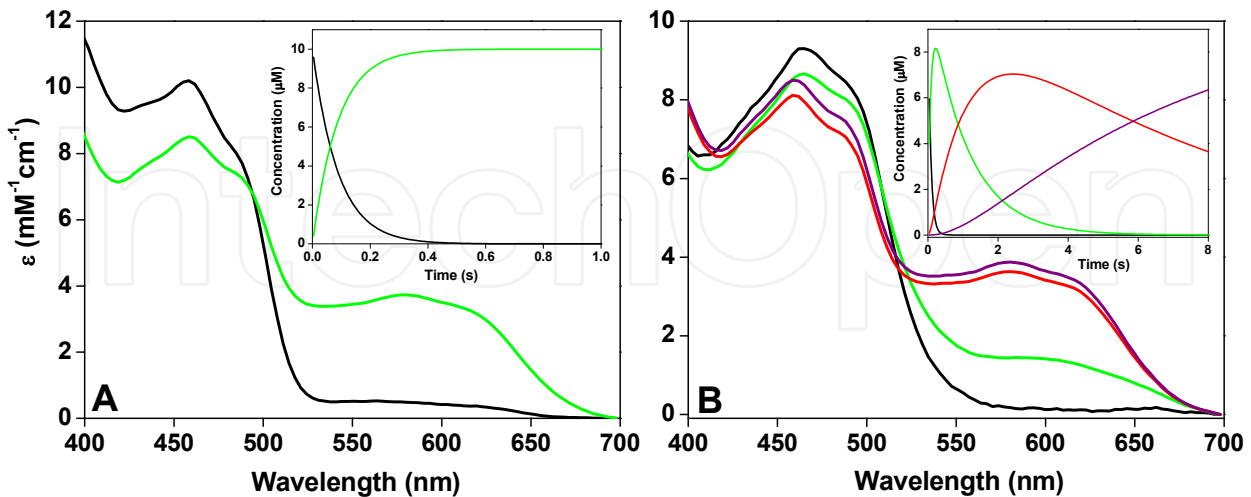

Fig. 7. Absorbance spectra for the pre-steady-state kinetically distinguishable intermediate species in the reaction of FNR_{ox} with (A) E16K/E61K Fld_{hq} and (B) E16K/E61K/D126K/D150K Fld_{hq}. The insets show the time evolution of these species. Species A, B, C and D species are shown in black, green, red and purple lines, respectively. Processes studied in 50 mM Tris/HCl, pH 8.0 at 12°C.

4. Spectral evolution of the electron transfer from FNR$_{hq}$ to Fld$_{ox}$

When FNR$_{hq}$ reacted with Fld$_{ox}$ an initial bleaching and displacement of the maximum from 464 nm (typical of Fld$_{ox}$) to 458 nm (maximum for FNR$_{ox}$) was observed, together with the appearance of a neutral semiquinone band (Fig. 8A). Then, absorbance increased in both the band-I and the semiquinone one (Fig. 8A and 8B). During the overall process only minor absorbance changes were detected in the Fld$_{ox/sq}$ isosbestic point (517 nm) at all the ionic strengths assayed, but an absorbance bleaching was initially observed at the FNR$_{ox/sq}$ one (507 nm) (Fig. 8B).
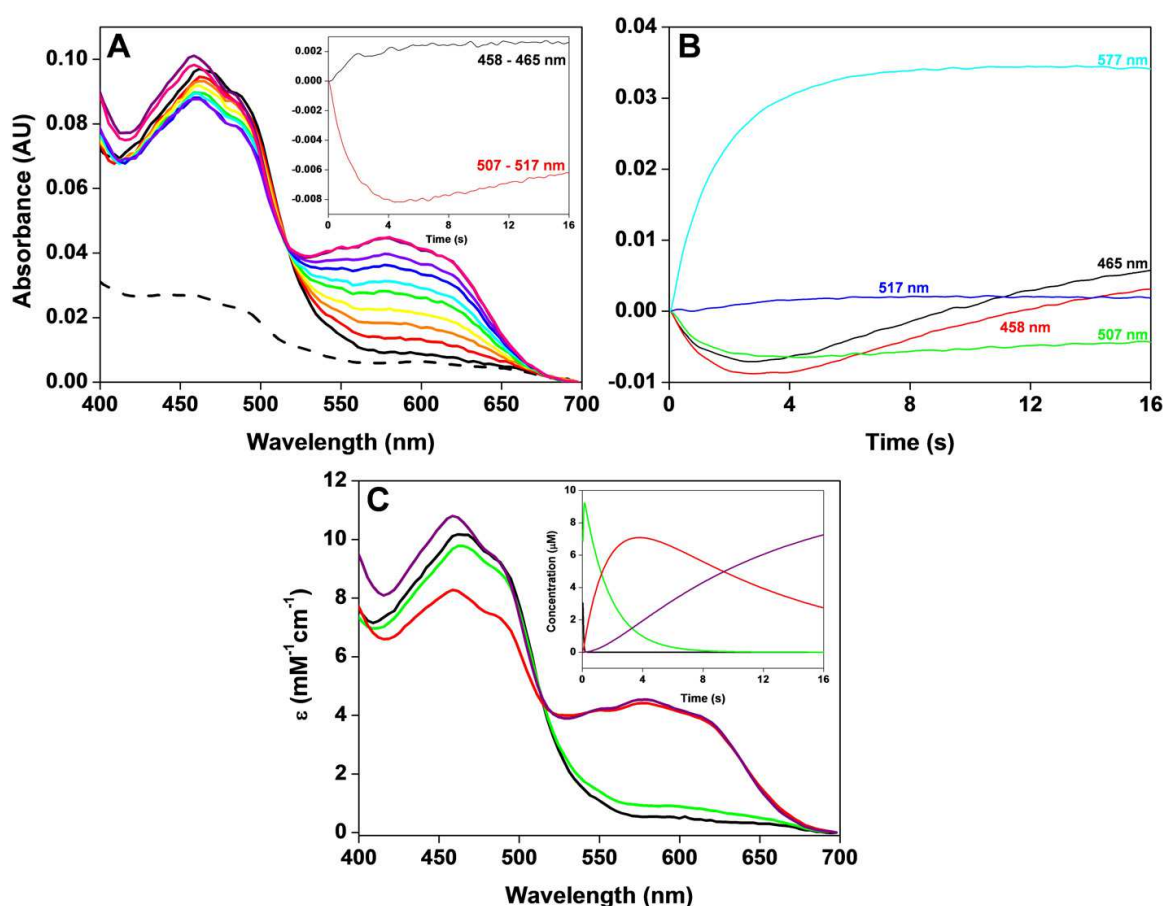

Fig. 8. Evolution of spectral changes observed during the reaction of Fld$_{ox}$ with FNR$_{hq}$. (A). Time course with spectra recorded at 0.03968, 0.2035, 0.4083, 0.695, 1.187, 1.555, 2.456, 3.521, 16.38 and 12.61 s after mixing. The spectrum of FNR$_{hq}$ before mixing is shown as a dashed line, and the first spectrum after mixing is in black. The inset shows kinetic traces at the indicated wavelengths. (B). Kinetics of absorbance changes observed at 458, 464, 507, 516 and 577 nm. (C). Absorbance spectra for the pre-steady-state kinetically distinguishable species obtained by global analysis. The inset shows the evolution of these species along the time. A, B, C and, D species are shown in black, green, red and purple lines, respectively. Processes studied in 50 mM Tris/HCl, pH 8.0, 100 mM NaCl at 12°C.

When globally analysed this reaction best fits to a three steps process (A → B → C → D) (Fig. 8C). Conversion of species A into B was relatively fast ($k_{A→B}$ >50 s^{-1}) with very little absorbance changes. Both species had FNR$_{hq}$ and Fld$_{ox}$ as the main components, but deviation of mathematical combination of individual redox spectra (Fig. 2) indicated their spectroscopic properties were modulated by the presence of each other. This suggests a number of FNR$_{hq}$ and Fld$_{ox}$ molecules must be forming a FNR$_{hq}$:Fld$_{ox}$ complex. This step appears, therefore, rather indicative of a protein-protein interaction or reorganisation event than of an ET one. B evolved to C in a relatively slow process (Table 1), in which the intensity of the band-I of the flavin gets decrease by ~20% and displaced to shorter wavelengths, whereas accumulation of semiquinone is produced (Fig. 8B). These observations are compatible with Fld$_{ox}$ being consumed and FNR$_{sq}$, Fld$_{sq}$ and FNR$_{ox}$ as the main components of species C. On conversion of C into D, there is an increment in the band-I absorption intensity (with the maximum at ~458 nm) and minor changes in the semiquinone band amplitude. This is consistent with FNR$_{ox}$ and Fld$_{sq}$ as the main components of D. The faster ET rates are observed at the lower ionic strength, but the ionic strength effect is much more moderated than for the reverse reaction (Fig. 9A). Reaction of FNR$_{hq}$ with Fld$_{ox}$ was also analysed at different protein-protein ratios showing similar behaviour and a linear dependence of $k_{B→C}$ and $k_{C→D}$ rates (Fig. 9B).
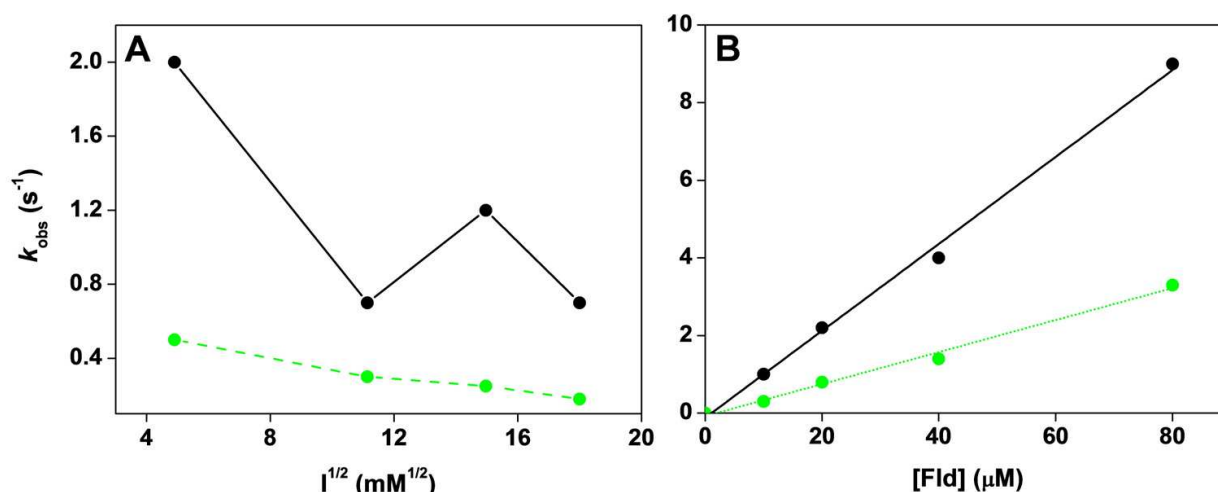

Fig. 9. (A). Ionic strength dependence of the apparent rate constants for the reduction of Fld$_{ox}$ by FNR$_{hq}$. The reaction was fit to a two-step process, $k_{B→C}$ (black) and $k_{C→D}$ (green). (B). Fld$_{ox}$ concentration dependence of the apparent rate constants for the reduction of Fld$_{ox}$ by FNR$_{hq}$ at I = 25 mM.

Reactions of FNR$_{hq}$ with E16K/E61K or E16K/E61K/D126K/D150K Fld$_{ox}$ variants showed similar features to the WT Fld (Fig. 10). Transformation of A into B appeared slightly slower for E16K/E61K ($k_{A→B}$ ~11 s^{-1}), while those species could not be resolved for E16K/E61K/D126K/D150K. These observations are in agreement with the 23-fold decrease and the absence of interaction reported for the complexes of E16K/E61K or E16K/E61K/D126K/D150K Fld$_{ox}$, respectively, with FNR$_{ox}$ (Goñi et al., 2009). B evolved to C in an ET process only 2-fold slower than for WT Fld$_{ox}$ (Table 1) and similarly consistent with FNR$_{sq}$ and Fld$_{sq}$ as the main components of C. On conversion of C into D, absorbance increments are observed in the band-I and the semiquinone band of the flavin, particularly

in the E16K/E61K/D126K/D150K Fld variant. This might be consistent with FNR_{sq} deproportionation into FNR_{ox} and FNR_{hq}, with the FNR_{hq} produced being able to reduce another Fld_{ox} molecule to the semiquinone state. Again processes of E301A FNR_{ox} with Fld_{hq} resembled those for the native proteins, with rate constants just slightly decreased and in agreement with previous reported data (Medina *et al.*, 1998).
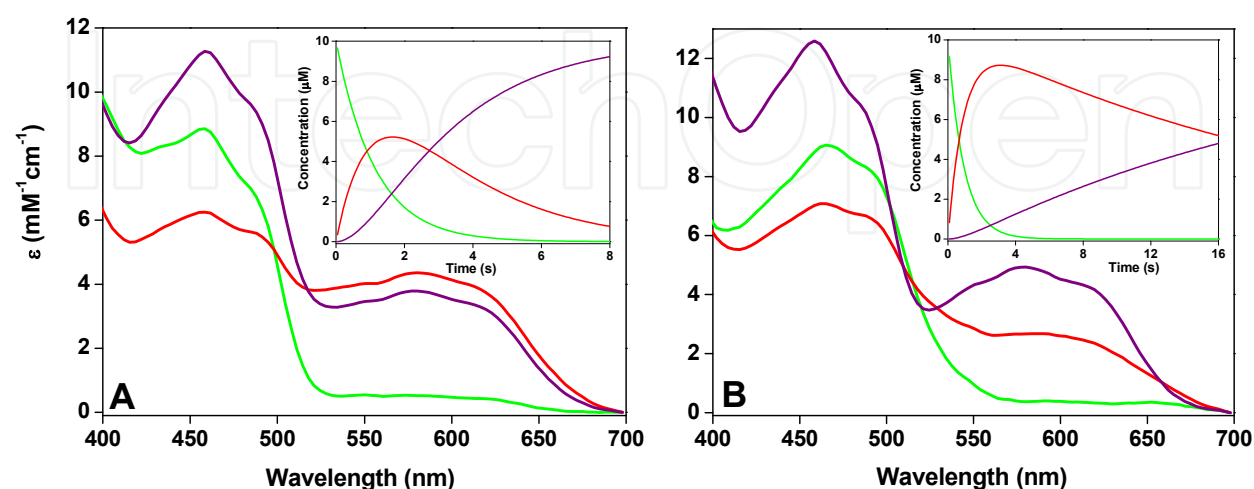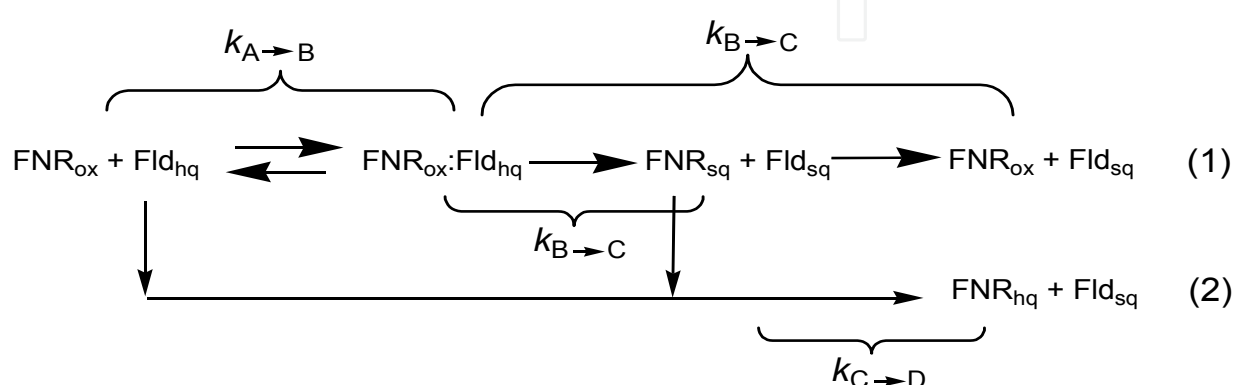

Fig. 10. Absorbance spectra for the pre-steady-state kinetically distinguishable species obtained by global analysis of the reaction of FNR_{hq} with (A) E16K/E61K Fld_{ox} and (B) E16K/E61K/D126K/D150K Fld_{ox}. Insets show the evolution of these species along the time. Intermediate B, C and D species are shown in green, red and, purple lines, respectively. Processes were studied in 50 mM Tris/HCl, pH 8.0, at 12ºC.

5. Insights into the electron transfer processes in the Fld:FNR system

The physiological ET from WT Fld_{hq} to WT FNR_{ox} was reported as a very fast process difficult to follow by single-wavelength stopped-flow methods. Nevertheless, this methodology resulted useful to study the processes for some FNR or Fld mutants with altered interaction or ET properties, but interpretation of the data was usually confuse due to the spectral similarities between the different oxido-reduction states of both proteins (Fig. 2) (Casaus *et al.*, 2002; Goñi *et al.*, 2008; Goñi *et al.*, 2009; Medina *et al.*, 1998; Nogués *et al.*, 2003; Nogués *et al.*, 2005). Analysis of mutants suggested that the reaction might take place in two steps interpreted as formation of the semiquinones of both proteins followed by further reduction of FNR_{sq} to the fully reduced state, with further accumulation of Fld_{sq} at the end of the reaction. Therefore, a similar behaviour was assumed for the WT system. In this work, we have taken advantage of stopped-flow with PDA detection to better evaluate the intermediate and final species in the equilibrium mixture during these ET processes for the reactions using the WT proteins and some of their mutants.

Analysis of the process for the reduction of WT FNR_{ox} by WT Fld_{hq}, under similar conditions to those so far reported at single-wavelengths, indicates that even using PDA it is difficult to extract conclusions for this ET process. The data suggest a very fast interaction (or collisional) step unable to be observed ($k_{A \to B}$), followed by an ET step than cannot be resolved from the subsequent equilibration to finally produce Fld_{sq} and FNR_{ox} (process (1) in Scheme 1). However, despite FNR_{sq} is hardly detected along the reaction, both semiquinones, Fld_{sq} and FNR_{sq}, must be initially produced. Moreover, FNR_{sq} does not

appear to be further reduced to FNR_{hq}, and apparently quickly relaxes to FNR_{ox}. Surprisingly, such behaviour was observed even when the overall ET reaction results slowed down by increasing the ionic strength. Thus, fast relaxation of the equilibrium distribution after the initial ET is produced with the consequent accumulation of FNR_{ox} and Fld_{sq}. Previous fast kinetic studies using laser flash photolysis indicated that ET from WT FNR_{sq} to WT Fld_{ox} is an extremely fast process ($k_{obs} \sim 7000$ s^{-1}), suggesting the produced FNR_{sq} will quickly react with any traces of Fld_{ox} producing Fld_{sq} and FNR_{ox} (Medina *et al.*, 1992). Moreover, the proper nature of the PDA experiment might also contribute to this effect, since the high intensity of the lamp simultaneously exciting a wavelength range might produce side energy transfer reactions.

$$
\begin{array}{l}
\overset{\displaystyle k_{A \to B}}{\overbrace{\phantom{FNR_{ox}+Fld_{hq} \rightleftharpoons FNR_{ox}:Fld_{hq}}}} \quad \overset{\displaystyle k_{B \to C}}{\overbrace{\phantom{FNR_{ox}:Fld_{hq} \longrightarrow FNR_{sq}+Fld_{sq} \longrightarrow FNR_{ox}+Fld_{sq}}}}
\end{array}
$$

$$FNR_{ox} + Fld_{hq} \rightleftharpoons FNR_{ox}{:}Fld_{hq} \longrightarrow FNR_{sq} + Fld_{sq} \longrightarrow FNR_{ox} + Fld_{sq} \quad (1)$$

$$\underset{\displaystyle k_{B \to C}}{\underbrace{\phantom{FNR_{ox}:Fld_{hq} \longrightarrow FNR_{sq}+Fld_{sq}}}}$$

$$\longrightarrow FNR_{hq} + Fld_{sq} \quad (2)$$

$$\underset{\displaystyle k_{C \to D}}{\underbrace{\phantom{FNR_{hq}+Fld_{sq}}}}$$

Scheme 1. Reaction pathways describing the processes observed for the reaction of FNR_{ox} with Fld_{hq} in the WT system (1) and with some of the Fld_{hq} mutants (2).
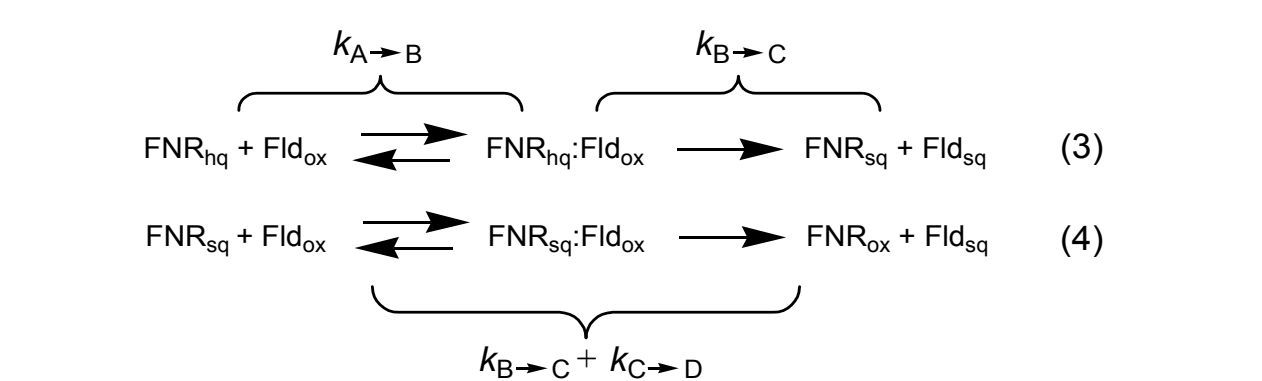
When reduction of E301A FNR_{ox} by Fld_{hq} was analysed a very similar behaviour to the WT one described the process, again suggesting quick FNR_{sq} deproportionation. When using the same methodology to analyse the process for two Fld mutants, with interaction and ET parameters considerably hindered (Goñi *et al.*, 2009), intermediates and products of the reaction were in agreement with the mechanism previously proposed using single-wavelength detection and with the final production of FNR_{hq} and Fld_{sq} under the assayed conditions (Scheme 1 reaction (2)). The PDA analysis additionally allowed improving the determination of the ET rates (Table 1). In these cases the initially produced FNR_{sq} appears unable to quickly react with traces of the Fld_{ox} mutants, preventing the quick relaxation after the initial ET. This effect can be explained since the $E_{ox/sq}$ for these Fld variants is more negative than in WT Fld, getting closer to the FNR $E_{ox/sq}$ and making ET from FNR_{sq} to Fld_{ox} less favourable from the thermodynamic point of view than in the WT reaction (Table 2). Therefore, our observations suggest that the stopped-flow methodology, independently of the detector, does not allow to identify the initial acceptance by WT or E301A FNR_{ox} of a single electron from WT Fld_{hq}, since under the experimental conditions (even upon increasing the ionic strength of the media) the subsequent relaxation of the putatively initially produced FNR_{sq} is faster than the initial ET process. Moreover, the products of this relaxation consist of a mixture of species that might not have physiological relevance within the *Anabaena* cell, where FNR_{sq} must be able to accept electrons from a second Fld_{hq} molecule.

The reverse ET reaction, FNR_{hq} with Fld_{ox} was reported as a slow process (when compared with the photosynthetic one) taking place in two sequential ET steps; production of both

flavoprotein semiquinones (reaction (3) in Scheme 2), followed by the reduction of a second Fld_{ox} molecule by the FNR_{sq} produced in the first step (reaction (4) in Scheme 2) (Casaus *et al.*, 2002; Medina *et al.*, 1998; Nogués *et al.*, 2005). The spectral evolutions acquired using the PDA detector confirm such mechanism, and allowed to improve the assignment of intermediates and the major contribution of apparent rate constants to particular steps of the process.

Fld form	$E_{ox/sq}$ (mV)	$E_{sq/hq}$ (mV)	$\Delta E_{ox/sq}$ - $\Delta E_{ox/sq}{}^{WT}$ (mV)	$\Delta E_{sq/hq}$ - $\Delta E_{sq/hq}{}^{WT}$ (mV)	$K_d{}^{FNRox:Fldox}$ (µM)
WT[a]	-256	-445	---	---	2.6
E16K/E61K[a]	-301	-390	-45	55	46
E16K/E61K/D126K/D150K[a]	-297	-391	-41	54	---
FNR form					
WT[b]	-325	-338	---	---	3[c]
E301A	-284[b]	-358[b]	41	-20	4[c]

Table 2. Midpoint reduction potentials for the different *Anabaena* Fld and FNR forms. Data obtained in 50 mM Tris/HCl at pH 8.0 and 25 °C for Fld[a] and at 10°C for FNR[b]. [a]Data from (Goñi *et al.*, 2009). [b]Data from (Faro *et al.*, 2002b). [c]Data from (Medina *et al.*, 1998).

$$k_{A \to B} \qquad\qquad k_{B \to C}$$

$$FNR_{hq} + Fld_{ox} \rightleftharpoons FNR_{hq}{:}Fld_{ox} \longrightarrow FNR_{sq} + Fld_{sq} \qquad (3)$$

$$FNR_{sq} + Fld_{ox} \rightleftharpoons FNR_{sq}{:}Fld_{ox} \longrightarrow FNR_{ox} + Fld_{sq} \qquad (4)$$

$$k_{B \to C} + k_{C \to D}$$

Scheme 2. Reaction pathways describing the processes observed for the reaction of the FNR_{hq} variants with the Fld_{ox} variants.

Thus, for the process with the E16K/E61K Fld variant, the step corresponding to complex formation-reorganisation was erroneously related with an ET step in a previous study. At the lowest ionic strength assayed our data indicate that E16K/E61K Fld_{ox} and, particularly, E16K/E61K/D126/D150K Fld_{ox} are still able to accept electrons from FNR_{ox} with apparent rates that only decreased by 2-fold and with final production of FNR_{ox} occurring in higher degree that in the WT system (Table 1, Fig. 8 and 10). Their slightly more negative $E_{ox/sq}$ values (Table 2) makes them poorer electron acceptors from FNR_{hq} than WT Fld and might explain the small differences in rates (Goñi *et al.*, 2009). Additionally, E301A FNR_{hq} is also able to pass electrons to Fld_{ox} with a rate 5-fold slower than WT (Table 1). This behaviour might be related with the very low stability of the semiquinone form in this FNR mutant (Table 2), that makes the formation of this intermediate state non-favourable (Medina *et al.*, 1998).

A biphasic dependence of the observed rate constants on the protein concentration has been reported for the ET reaction from Fd to FNR (Fig. 4), and associated with the appearance of

an optimum ionic strength value and with the electrostatic stabilisation at low ionic strengths of non-optimal orientations within the intermediate ET complex. Thus, specific electrostatic and hydrophobic interactions play an important role in these association and dissociation processes, as well as in the rearrangement of the complex (Faro *et al.*, 2002a; Hurley *et al.*, 2006; Martínez-Júlvez *et al.*, 1998; Martínez-Júlvez *et al.*, 1999; Martínez-Júlvez *et al.*, 2001; Medina & Gómez-Moreno, 2004; Morales *et al.*, 2000; Nogués *et al.*, 2003). Despite some residues on the FNR surface are critical for the interaction with Fld and it is accepted that FNR interacts using the same region with Fld and Fd (Hurley *et al.*, 2002; Martínez-Júlvez *et al.*, 1999), the bell-shaped profile for the ionic strength dependence is not reproduced for ET reactions between FNR and Fld (Fig. 4). A strong deleterious influence of the ionic strength is observed on the overall ET process between Fld and FNR, particularly in the photosynthetic direction (Fig. 4 and 9A). This suggests re-arrangement of the initial FNR:Fld interaction either does not take place or does not increase the efficiency of the system, while at lower ionic strength the electrostatic interactions contribute to produce more efficient orientations between the flavin cofactors.

Biochemical and docking studies suggested that the FNR:Fld interaction does not rely on a precise complementary surface of the reacting molecules. Thus, WT Fld might adopt different orientations on the FNR surface without significantly altering the relative disposition and contact between the FMN and FAD groups of Fld and FNR and, therefore, the distance between their methyl groups (Fig. 11A) (Goñi *et al.*, 2009; Medina *et al.*, 2008; Medina, 2009). Those studies suggested the molecular dipole moment alignment as one of the major determinants for the efficiency of this system (Fig. 11B). However, kinetic
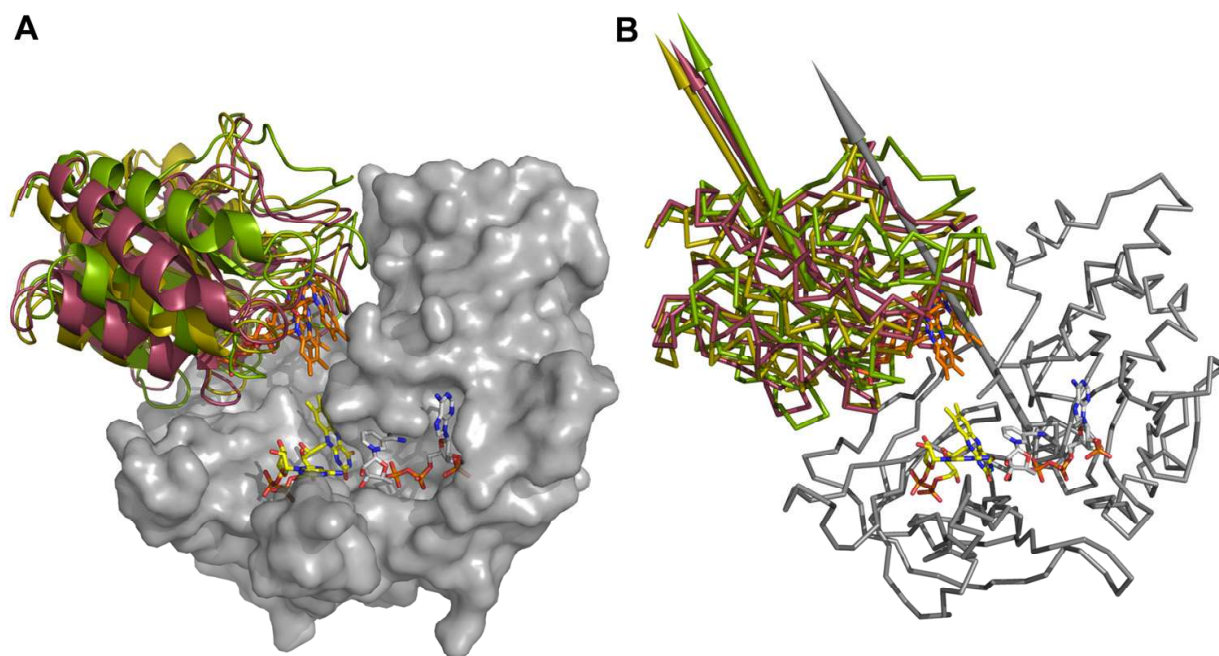

Fig. 11. (A). Model for the interaction of Fld and FNR. The figure shows several positions determined by docking of Fld onto the FNR surface. (B). Magnitude and orientation of the dipole moment of Fld and FNR in the model.

parameters reported to the date for these processes were only obtained at low ionic strength (~0.03 M), conditions far away from those found in the thylakoid (0.15-0.3 M (Durán *et al.*, 2006)). Our data suggest that at physiological ionic strengths the ET efficiency, particularly in the photosynthetic direction, will be considerably hindered with regard to the data reported *in vitro* at low ionic strengths. The ionic strength will shield the dipole moment alignment contribution, making it just one additional contribution to proteins encounter. Among those contributions we might include electrostatic and hydrophobic interactions imposed by the thylakoid membrane, physical diffusional parameters and molecular crowding inside the cell. It is also worth to note that increasing the ionic strength makes reduction of FNR by Fld_{hq} only 4-8 times faster than the reverse process (Compare Fig. 4A and 9A). Thus, shielding the effect of the dipole moment appears to have a larger impact in producing the competent ET orientation between the redox centres in the $FNR_{ox}:Fld_{hq}$ complex than in the $FNR_{hq}:Fld_{ox}$ one. In other words, it reduces the probability of obtaining the best $FNR_{ox}:Fld_{hq}$ orientations for ET.

The Fld mutants here studied, particularly E16K/E61K/D126/D150K, have lost the ability to efficiently reduce FNR (Table 1). More positive $E_{sq/hq}$ values (Table 2) might somehow contribute to this behaviour, but previous studies suggested the introduced mutations induced changes in the Fld electrostatic potential surfaces, as well as in the orientation and magnitude of the Fld molecular dipole moment (Goñi *et al.*, 2009). Despite the thermodynamic parameters favour the process, the observed reaction might only correlate with a collisional-type reaction. Therefore, it could exit the possibility that steering of the dipole moment contribution might produce a positive effect on the overall ET process. However, our analysis also shows that the increasing of the ionic strength again had a deleterious effect in the ET processes from these Fld_{hq} mutants. Thus, electrostatic and hydrophobic interactions and the dipole moment still must contribute to the formation of productive interactions between both proteins at physiological ionic strengths. *In vivo* the presence of other proteins competing for Fld_{hq} might also result in changes to electron channelling into distinct pathways. When going to physiological conditions Fld interaction with FNR is confirmed to be less specific than that of Fd. Subtle changes at the isoalloxazine environment influence the Fld binding abilities and modulate the ET processes by producing different orientations and distances between the redox centres. Therefore, ET reactions involving Fld might not have as much specific interaction requirements as other reactions involving protein-protein interactions. Thus, the bound state could be formed by dynamic ensembles instead of single conformations as has already been proposed for this system (Fig. 11) (Goñi *et al.*, 2009; Medina *et al.*, 2008) and also observed in other ET systems (Crowley & Carrondo, 2004; Worrall *et al.*, 2003). This further confirms previous studies suggesting that Fld interacts with different structural partners through non-specific interactions, which in turn decreased the potential efficiency in ET that could achieve if unique and more favourable orientations were produced with a reduced number of partners. Heterogeneity of ET kinetics is an intrinsic property of Fld oxido-reduction processes, and can be most probably ascribed to different conformations of FNR:Fld complexes (Medina *et al.*, 2008; Sétif, 2001). During Fld-dependent photosynthetic ET the Fld molecule must pivot between its docking sites in PSI and in FNR. Formation of transient complexes of Fld with FNR *in vivo* is useful during this process, though not critical, for promoting efficient reduction of Fld and FNR and for avoiding reduction of oxygen by the donor redox centres (Goñi *et al.*, 2008; Goñi *et al.*, 2009; Hurley *et al.*, 2006; Sétif, 2001, 2006).

6. Conclusion

Single-wavelength fast kinetic stopped-flow methods have been widely used for the analysis of the mechanisms involving transient binding and ET between Fld and FNR. However, this methodology did not allow to un-ambiguously identifying the intermediate and final compounds of the reactions. PDA detection combined with fast kinetic stopped-flow methods results useful to better understand the mechanisms involving transient binding and ET between Fld and FNR. Despite the high similarity among the spectra for the same redox states within both proteins, the methodology here used allowed identifying the composition of the intermediate species and final species of the reactions, as long as the kinetics fits in the measurable instrumental time. The mechanism of these inter-flavin ET reactions is revisited, evaluating the evolution of the reaction along the time within a wavelength spectral range by using a PDA detector. Additionally, our analysis of the dependence of the inter-flavin ET mechanism on the ionic strength suggest that, under physiological conditions, the electrostatic alignment contributes to the overall orientation but it is not anymore the major determinant of the orientation of Fld on the protein partner surface. Additionally, the presence of the coenzyme reveals a complex modulation of the process.

7. Acknowledgment

8. References

Arakaki, A. K., Ceccarelli, E. A. & Carrillo, N. (1997). Plant-type ferredoxin-NADP⁺ reductases: a basal structural framework and a multiplicity of functions. *Faseb J*. Vol.11, No.2, pp. 133-140, ISSN 0892-6638.

Batie, C. J. & Kamin, H. (1984a). Electron transfer by ferredoxin:NADP⁺ reductase. Rapid-reaction evidence for participation of a ternary complex. *J Biol Chem*. Vol.259, No.19, pp. 11976-11985, ISSN 0021-9258.

Batie, C. J. & Kamin, H. (1984b). Ferredoxin:NADP⁺ oxidoreductase. Equilibria in binary and ternary complexes with NADP⁺ and ferredoxin. *J Biol Chem*. Vol.259, No.14, pp. 8832-8839, ISSN 0021-9258.

Bottin, H. & Lagoutte, B. (1992). Ferredoxin and flavodoxin from the cyanobacterium *Synechocystis* sp PCC 6803. *BBA-Bioenergetics*. Vol.1101, No.1, pp. 48-56, ISSN 0005-2728.

Brenner, S., Hay, S., Munro, A. W. & Scrutton, N. S. (2008). Inter-flavin electron transfer in cytochrome P450 reductase - effects of solvent and pH identify hidden complexity in mechanism. *Febs J*. Vol.275, No.18, pp. 4540-4557, ISSN 1742-464X.

Carrillo, N. & Ceccarelli, E. A. (2003). Open questions in ferredoxin-NADP⁺ reductase catalytic mechanism. *Eur J Biochem*. Vol.270, No.9, pp. 1900-1915, ISSN 0014-2956.

Casaus, J. L., Navarro, J. A., Hervás, M., Lostao, A., De la Rosa, M. A., Gómez-Moreno, C., Sancho, J. & Medina, M. (2002). *Anabaena* sp. PCC 7119 flavodoxin as electron

carrier from photosystem I to ferredoxin-NADP⁺ reductase. Role of Trp(57) and Tyr(94). *J Biol Chem*. Vol.277, No.25, pp. 22338-22344, ISSN 0021-9258.

Crowley, P. B. & Carrondo, M. A. (2004). The architecture of the binding site in redox protein complexes: implications for fast dissociation. *Proteins*. Vol.55, No.3, pp. 603-612, ISSN 0887-3585.

Dumit, V. I., Essigke, T., Cortez, N. & Ullmann, G. M. (2010). Mechanistic insights into ferredoxin-NADP(H) reductase catalysis involving the conserved glutamate in the active site. *J Mol Biol*. Vol.397, No.3, pp. 814-825, ISSN 0022-2836.

Durán, R. V., Hervás, M., de la Cerda, B., de la Rosa, M. A. & Navarro, J. A. (2006). A laser flash-induced kinetic analysis of in vivo photosystem I reduction by site-directed mutants of plastocyanin and cytochrome c_6 in *Synechocystis sp.* PCC 6803. *Biochemistry*. Vol.45, No.3, pp. 1054-1060, ISSN 0006-2960.

Faro, M., Frago, S., Mayoral, T., Hermoso, J. A., Sanz-Aparicio, J., Gómez-Moreno, C. & Medina, M. (2002a). Probing the role of glutamic acid 139 of *Anabaena* ferredoxin-NADP⁺ reductase in the interaction with substrates. *Eur J Biochem*. Vol.269, No.20, pp. 4938-4947, ISSN 0014-2956.

Faro, M., Gómez-Moreno, C., Stankovich, M. & Medina, M. (2002b). Role of critical charged residues in reduction potential modulation of ferredoxin-NADP⁺ reductase. *Eur J Biochem*. Vol.269, No.11, pp. 2656-2661, ISSN 0014-2956.

Frago, S., Goñi, G., Herguedas, B., Peregrina, J. R., Serrano, A., Pérez-Dorado, I., Molina, R., Gómez-Moreno, C., Hermoso, J. A., Martínez-Júlvez, M., Mayhew, S. G. & Medina, M. (2007). Tuning of the FMN binding and oxido-reduction properties by neighboring side chains in *Anabaena* flavodoxin. *Arch Biochem Biophys*. Vol.467, No.2, pp. 206-217, ISSN 0003-9861.

Frago, S., Lans, I., Navarro, J. A., Hervás, M., Edmondson, D. E., de la Rosa, M. A., Gómez-Moreno, C., Mayhew, S. G. & Medina, M. (2010). Dual role of FMN in flavodoxin function: Electron transfer cofactor and modulation of the protein-protein interaction surface. *BBA-Bioenergetics*. Vol.1797, No.2, pp. 262-271, ISSN 0005-2728.

Golbeck, J. H., Ed. (2006). *Photosystem I. The light-driven platocyanin:ferredoxin oxidoreductase*, Springer, ISBN 1-4020-4255-8, Dordrecht, The Netherlands.

Goñi, G., Serrano, A., Frago, S., Hervás, M., Peregrina, J. R., de la Rosa, M. A., Gómez-Moreno, C., Navarro, J. A. & Medina, M. (2008). Flavodoxin-mediated electron transfer from photosystem I to ferredoxin-NADP⁺ reductase in *Anabaena*: role of flavodoxin hydrophobic residues in protein-protein interactions. *Biochemistry*. Vol.47, No.4, pp. 1207-1217, ISSN 0006-2960.

Goñi, G., Herguedas, B., Hervás, M., Peregrina, J. R., de la Rosa, M. A., Gómez-Moreno, C., Navarro, J. A., Hermoso, J. A., Martínez-Júlvez, M. & Medina, M. (2009). Flavodoxin: A compromise between efficiency and versatility in the electron transfer from Photosystem I to Ferredoxin-NADP⁺ reductase. *BBA-Bioenergetics*. Vol.1787, No.3, pp. 144-154, ISSN 0005-2728.

Hurley, J. K., Morales, R., Martínez-Júlvez, M., Brodie, T. B., Medina, M., Gómez-Moreno, C. & Tollin, G. (2002). Structure-function relationships in *Anabaena* ferredoxin/ferredoxin-NADP⁺ reductase electron transfer: insights from site-directed mutagenesis, transient absorption spectroscopy and X-ray crystallography. *BBA-Bioenergetics*. Vol.1554, No.1-2, pp. 5-21, ISSN 0005-2728.

Hurley, J. K., Tollin, G., Medina, M. & Gómez-Moreno, C. (2006). Electron transfer from ferredoxin and flavodoxin to ferredoxin-NADP$^+$ reductase, In: *Photosystem I. The light-driven platocyanin:ferredoxin oxidoreductase*, J. H. Golbeck (Ed.), pp. 455-476, Springer, ISBN 1-4020-4255-8, Dordrecht, The Netherlands.

Martínez-Júlvez, M., Medina, M., Hurley, J. K., Hafezi, R., Brodie, T. B., Tollin, G. & Gómez-Moreno, C. (1998). Lys75 of *Anabaena* ferredoxin-NADP$^+$ reductase is a critical residue for binding ferredoxin and flavodoxin during electron transfer. *Biochemistry*. Vol.37, No.39, pp. 13604-13613, ISSN 0006-2960.

Martínez-Júlvez, M., Medina, M. & Gómez-Moreno, C. (1999). Ferredoxin-NADP$^+$ reductase uses the same site for the interaction with ferredoxin and flavodoxin. *J Biol Inorg Chem*. Vol.4, No.5, pp. 568-578, ISSN 0949-8257.

Martínez-Júlvez, M., Nogués, I., Faro, M., Hurley, J. K., Brodie, T. B., Mayoral, T., Sanz-Aparicio, J., Hermoso, J. A., Stankovich, M. T., Medina, M., Tollin, G. & Gómez-Moreno, C. (2001). Role of a cluster of hydrophobic residues near the FAD cofactor in *Anabaena* PCC 7119 ferredoxin-NADP$^+$ reductase for optimal complex formation and electron transfer to ferredoxin. *J Biol Chem*. Vol.276, No.29, pp. 27498-27510, ISSN 0021-9258.

Martínez-Júlvez, M., Medina, M. & Velázquez-Campoy, A. (2009). Binding thermodynamics of ferredoxin:NADP$^+$ reductase: two different protein substrates and one energetics. *Biophys J*. Vol.96, No.12, pp. 4966-4975, ISSN 0006-3495.

Medina, M., Gómez-Moreno, C. & Tollin, G. (1992). Effects of chemical modification of *Anabaena* flavodoxin and ferredoxin-NADP$^+$ reductase on the kinetics of interprotein electron transfer reactions. *Eur J Biochem*. Vol.210, No.2, pp. 577-583, ISSN 0014-2956.

Medina, M., Martínez-Júlvez, M., Hurley, J. K., Tollin, G. & Gómez-Moreno, C. (1998). Involvement of glutamic acid 301 in the catalytic mechanism of ferredoxin-NADP$^+$ reductase from *Anabaena* PCC 7119. *Biochemistry*. Vol.37, No.9, pp. 2715-2728, ISSN 0006-2960.

Medina, M. & Gómez-Moreno, C. (2004). Interaction of ferredoxin-NADP$^+$ reductase with its substrates: Optimal interaction for efficient electron transfer. *Photosynth Res*. Vol.79, No.2, pp. 113-131, ISSN 0166-8595.

Medina, M., Abagyan, R., Gómez-Moreno, C. & Fernández-Recio, J. (2008). Docking analysis of transient complexes: interaction of ferredoxin-NADP$^+$ reductase with ferredoxin and flavodoxin. *Proteins*. Vol.72, No.3, pp. 848-862, ISSN 0887-3585.

Medina, M. (2009). Structural and mechanistic aspects of flavoproteins: Photosynthetic electron transfer from photosystem I to NADP$^+$. *Febs J*. Vol.276, No.15, pp. 3942-3958, ISSN 1742-464X.

Morales, R., Charon, M. H., Kachalova, G., Serre, L., Medina, M., Gómez-Moreno, C. & Frey, M. (2000). A redox-dependent interaction between two electron-transfer partners involved in photosynthesis. *EMBO Rep*. Vol.1, No.3, pp. 271-276, ISSN 1469-221X.

Müller, F., Ed. (1991). *Chemistry and Biochemistry of Flavoenzymes*, CRC Press, ISBN 0-8493-4393-3 Boca Raton, Florida.

Nogués, I., Martínez-Júlvez, M., Navarro, J. A., Hervás, M., Armenteros, L., de la Rosa, M. A., Brodie, T. B., Hurley, J. K., Tollin, G., Gómez-Moreno, C. & Medina, M. (2003). Role of hydrophobic interactions in the flavodoxin mediated electron transfer from

photosystem I to ferredoxin-NADP$^+$ reductase in *Anabaena* PCC 7119. *Biochemistry*. Vol.42, No.7, pp. 2036-2045, ISSN 0006-2960.

Nogués, I., Tejero, J., Hurley, J. K., Paladini, D., Frago, S., Tollin, G., Mayhew, S. G., Gómez-Moreno, C., Ceccarelli, E. A., Carrillo, N. & Medina, M. (2004). Role of the C-terminal tyrosine of ferredoxin-nicotinamide adenine dinucleotide phosphate reductase in the electron transfer processes with its protein partners ferredoxin and flavodoxin. *Biochemistry*. Vol.43, No.20, pp. 6127-6137, ISSN 0006-2960.

Nogués, I., Hervás, M., Peregrina, J. R., Navarro, J. A., de la Rosa, M. A., Gómez-Moreno, C. & Medina, M. (2005). *Anabaena* flavodoxin as an electron carrier from photosystem I to ferredoxin-NADP$^+$ reductase. Role of flavodoxin residues in protein-protein interaction and electron transfer. *Biochemistry*. Vol.44, No.1, pp. 97-104, ISSN 0006-2960.

Sancho, J., Medina, M. & Gómez-Moreno, C. (1990). Arginyl groups involved in the binding of *Anabaena* ferredoxin-NADP$^+$ reductase to NADP$^+$ and to ferredoxin. *Eur J Biochem*. Vol.187, No.1, pp. 39-48, ISSN 0014-2956.

Sétif, P. (2001). Ferredoxin and flavodoxin reduction by photosystem I. *BBA-Bioenergetics*. Vol.1507, No.1-3, pp. 161-179, ISSN 0005-2728.

Sétif, P. (2006). Electron transfer from the bound iron-sulfur clusters to ferredoxin/flavodoxin: kinetic and structural properties of ferredoxin/flavodoxin reduction by photosystem I, In: *Photosystem I. The light-driven platocyanin:ferredoxin oxidoreductase*, J. H. Golbeck (Ed.), pp. 439-454, Springer, ISBN 1-4020-4255-8, Dordrecht, The Netherlands.

Tejero, J., Martínez-Júlvez, M., Mayoral, T., Luquita, A., Sanz-Aparicio, J., Hermoso, J. A., Hurley, J. K., Tollin, G., Gómez-Moreno, C. & Medina, M. (2003). Involvement of the pyrophosphate and the 2'-phosphate binding regions of ferredoxin-NADP$^+$ reductase in coenzyme specificity. *J Biol Chem*. Vol.278, No.49, pp. 49203-49214, ISSN 0021-9258.

Tejero, J., Pérez-Dorado, I., Maya, C., Martínez-Júlvez, M., Sanz-Aparicio, J., Gómez-Moreno, C., Hermoso, J. A. & Medina, M. (2005). C-terminal tyrosine of ferredoxin-NADP$^+$ reductase in hydride transfer processes with NAD(P)$^+$/H. *Biochemistry*. Vol.44, No.41, pp. 13477-13490, ISSN 0006-2960.

Tejero, J., Peregrina, J. R., Martínez-Júlvez, M., Gutierrez, A., Gómez-Moreno, C., Scrutton, N. S. & Medina, M. (2007). Catalytic mechanism of hydride transfer between NADP$^+$/H and ferredoxin-NADP$^+$ reductase from *Anabaena* PCC 7119. *Arch Biochem Biophys*. Vol.459, No.1, pp. 79-90, ISSN 0003-9861.

Velázquez-Campoy, A., Goñi, G., Peregrina, J. R. & Medina, M. (2006). Exact analysis of heterotropic interactions in proteins: Characterization of cooperative ligand binding by isothermal titration calorimetry. *Biophys J*. Vol.91, No.5, pp. 1887-1904, ISSN 0006-3495.

Wolthers, K. R. & Scrutton, N. S. (2004). Electron transfer in human methionine synthase reductase studied by stopped-flow spectrophotometry. *Biochemistry*. Vol.43, No.2, pp. 490-500, ISSN 0006-2960.

Worrall, J. A., Reinle, W., Bernhardt, R. & Ubbink, M. (2003). Transient protein interactions studied by NMR spectroscopy: the case of cytochrome *c* and adrenodoxin. *Biochemistry*. Vol.42, No.23, pp. 7068-7076, ISSN 0006-2960.
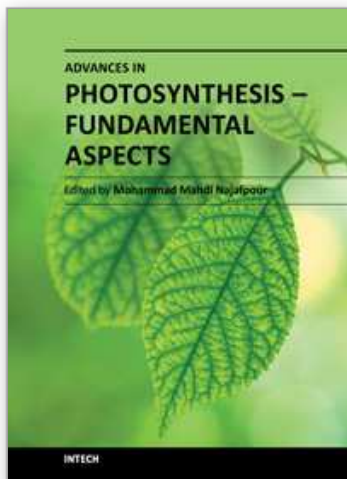
Advances in Photosynthesis - Fundamental Aspects

Edited by Dr Mohammad Najafpour

Photosynthesis is one of the most important reactions on Earth. It is a scientific field that is the topic of many research groups. This book is aimed at providing the fundamental aspects of photosynthesis, and the results collected from different research groups. There are three sections in this book: light and photosynthesis, the path of carbon in photosynthesis, and special topics in photosynthesis. In each section important topics in the subject are discussed and (or) reviewed by experts in each book chapter.

How to reference

In order to correctly reference this scholarly work, feel free to copy and paste the following:

INTECH

open science | open minds